Dimerization of the cytokine receptors gp130 and LIFR analysed in single cells

Bernd Giese*, Christoph Roderburg*, Michael Sommerauer, Saskia B. Wortmann, Silke Metz, Peter C. Heinrich and Gerhard Müller-Newen‡

Institut für Biochemie, Universitätsklinikum RWTH Aachen, Pauwelsstraße 30, 52074 Aachen, Germany

*These authors contributed equally to this work

‡Author for correspondence (e-mail: mueller-newen@rwth-aachen.de)

Accepted 09 August 2005
Journal of Cell Science 118, 5129-5140 Published by The Company of Biologists 2005
doi:10.1242/jcs.02628

Summary

The cytokine receptor gp130 is the shared signalling subunit of the IL-6-type cytokines. Interleukin-6 (IL-6) signals through gp130 homodimers whereas leukaemia inhibitory factor (LIF) exerts its action through a heterodimer of gp130 and the LIF receptor (LIFR). Related haematopoietic receptors such as the erythropoietin receptor have been described as preformed dimers in the plasma membrane. Here we investigated gp130 homodimerization and heterodimerization with the LIFR by fluorescence resonance energy transfer (FRET) and bimolecular fluorescence complementation (BiFC). We detected a FRET signal between YFP- and CFP-tagged gp130 at the plasma membrane of unstimulated cells that does not increase upon IL-6 stimulation. However, FRET between YFP-tagged gp130 and CFP-tagged LIFR considerably increased upon LIF stimulation. Using a BiFC approach that detects stable interactions we show that fluorescence complementation of gp130 constructs tagged with matching 'halves' of fluorescent proteins increases upon IL-6 stimulation. Taken together, these findings suggest that transient gp130 homodimers on the plasma membrane are stabilized by IL-6 whereas heterodimerization of gp130 with the LIFR is mainly triggered by the ligand. This view is supported by the observation that the simultaneous action of two IL-6 binding domains on two gp130 molecules is required to efficiently recruit a fluorescent IL-6 (YFP-IL-6) to the plasma membrane.

Key words: Cytokine receptor, Gp130, LIFR, Dimerization, FRET, BiFC

Introduction

Cytokines are important mediators of intercellular communication in higher organisms. The subfamily of haematopoietic cytokines plays a central role in the regulation of haematopoiesis and the immune response (Wells and de Vos, 1996). From knockout studies, it became evident that these mediators are also involved in the regulation of other fundamental biological processes such as embryonic development (Yoshida et al., 1996) and fertility (Robb et al., 1998; Stewart et al., 1992). In line with their biological activities, dysregulation of haematopoietic cytokine signalling contributes significantly to acute and chronic inflammation, immune deficiencies and cancer progression.

Together with interferons and cytokines of the IL-10 family, the haematopoietic cytokines build up the large family of helical cytokines (Boulay et al., 2003). Whereas interferons and IL-10 family cytokines signal through class II cytokine receptors, the haematopoietic cytokines use class I cytokine receptors. The structural hallmark of these class I or haematopoietic cytokine receptors is a tandem array of fibronectin type III-like (FNIII) domains termed cytokine binding module (CBM) or cytokine receptor homology region (CHR) (Wells and de Vos, 1996). The N-terminal FNIII domain is stabilized by four conserved cysteine residues forming two disulfide bonds, the C-terminal FNIII domain contains a highly conserved WSXWS motif. The extracellular part of 'short cytokine receptors' such as the erythropoietin (Epo) receptor or the growth hormone (GH) receptor consists only of a single CBM. 'Tall cytokine receptors' such as gp130 or the leukaemia inhibitory factor (LIF) receptor contain additional FNIII or Ig-like domains.

Class I and class II cytokine receptors signal through the Jak/STAT pathway (Ihle, 1995). The membrane proximal cytoplasmic part of these receptors is constitutively and stably associated with Janus tyrosine kinases (Jaks) (Giese et al., 2003). Upon cytokine binding to the extracellular part of the receptor, the cytoplasmic Jaks become activated by tyrosine phosphorylation. The activated Jaks phosphorylate tyrosine residues in the membrane distal cytoplasmic part of the receptor and the phosphotyrosine motifs are docking sites for signalling molecules containing SH2 or PTB domains. Most importantly, signal transducer and activator of transcription (STAT) proteins are recruited by their SH2 domain to specific phosphotyrosine motifs. Subsequently the Jaks phosphorylate the STATs at a single tyrosine residue leading to the release of STAT dimers from the receptor and their translocation to the nucleus where they activate target genes.

How exactly cytokine binding leads to receptor activation, i.e. triggering of the Jak/STAT pathway is an unresolved issue. Much progress has been made in the understanding of the

interaction of haematopoietic cytokines with their receptors. The growth hormone paradigm has been derived from the X-ray structure of GH bound to the soluble GH receptor (GHR) (de Vos et al., 1992). Two surface areas termed site I and site II of a single GH molecule bind to two identical receptor subunits leading to the idea that ligand-induced receptor dimerization is the main trigger for the signal transduction cascade. Studies on the related Epo/EpoR system revealed that an inactive EpoR dimer is formed by an artificial antagonistic peptide (Livnah et al., 1998). Thus, receptor dimerization does not necessarily lead to receptor activation. This idea was supported by experimental evidence suggesting that the EpoR exists as a preformed, inactive receptor dimer in the plasma membrane (Livnah et al., 1999). In this situation, instead of triggering dimerization, the ligand switches the receptor from an inactive to an active dimer conformation. Receptor pre-association has also been described for other receptors spanning the membrane only once (Jiang and Hunter, 1999).

Epo is the only known ligand for the EpoR. Besides such monospecific receptors, shared haematopoietic cytokine receptors exist which recognize several cytokines (Boulanger and Garcia, 2004). Three receptor systems are known, that are based on a central shared receptor subunit. The common beta chain (βc) is used by the cytokines IL-3, IL-5 and GM-CSF, the common gamma chain (γc) recognizes IL-2, IL-4, IL-7, IL-9, IL-15 and IL-21 whereas gp130 is the most promiscuous cytokine receptor involved in the binding of nine different cytokines (Bravo and Heath, 2000). These IL-6-type cytokines signal either through gp130 homodimers (IL-6, IL-11) or through heterodimers of gp130 and the LIFR (LIF, CNTF, CT-1, CLC, NP), heterodimers of gp130 and the OSMR (OSM) and heterodimers of gp130 and the IL-27R/WSX-1 (IL-27) (Heinrich et al., 2003). In such a scenario a stable preformed gp130 homodimer would greatly facilitate IL-6 and IL-11 signalling but at the same time would prevent signalling by the cytokines that require receptor heterodimerization. Conversely, stable preformed heterodimers would discriminate against signalling through gp130 homodimers.

The extracellular part of gp130 consists of six domains: an Ig-like domain (D1) is followed by the CBM (D2 and D3) and three further FNIII domains (D4-D6) (Hibi et al., 1990). In LIF-induced heterodimerization with the LIFR, only the CBM of gp130 contacts LIF (Hammacher et al., 1998; Timmermann et al., 2000). The LIFR contributes mainly with its Ig-like domain to LIF binding (Owczarek et al., 1997). Receptor assembly in response to IL-6 is more complicated. Activation of gp130 homodimers by IL-6 requires binding of IL-6 to a specific α-receptor (IL-6Rα) (Taga et al., 1989), which does not contribute to the intracellular signal transduction cascade. Cells that express gp130 but lack IL-6Rα expression can be stimulated by the combination of IL-6 and soluble IL-6Rα (sIL-6Rα) (Taga et al., 1989). The complex of IL-6Rα or sIL-6Rα bound to site I of IL-6 provides two gp130 binding sites (termed site II and site III). In the final hexameric receptor complex two IL-6/IL-6Rα heterodimers are bound to the gp130 homodimer (Boulanger et al., 2003b). One IL-6 molecule contacts with its site II the CBM of one gp130 and with its site III the Ig-like domain of the second gp130. The same is true in a reciprocal fashion for the second IL-6 molecule leading to a highly symmetrical complex.

In this report we investigate gp130 homodimerization and heterodimerization of gp130 with the LIFR in unstimulated and cytokine (IL-6 or LIF) stimulated cells. As discussed for other receptors (Jiang and Hunter, 1999), putative receptor/receptor interactions could be dominated by contacts of the transmembrane regions that require an intact plasma membrane. Furthermore, pre-association of receptors by weak protein-protein interactions could be disrupted by solubilization of the membrane. Therefore, we decided to study receptor oligomerization at the plasma membrane of single, intact cells by fluorescence resonance energy transfer (FRET) and bimolecular fluorescence complementation (BiFC). We found, that gp130 forms transient homodimers that are stabilized by addition of the ligand. Heterodimerization of gp130 with the LIFR, however, is mainly triggered by the ligand. We present a model of receptor assembly that takes into account the different ligand-binding characteristics of gp130 homodimers and gp130/LIFR heterodimers.

Materials and Methods

Proteins, chemicals, cell culture and transfection

Enzymes were purchased from Roche (Penzberg, Germany), DMEM and antibiotics from Cambrex BioScience (Belgium) and Invitrogen (USA); Sf-900II medium was obtained from Gibco (USA), FCS from CytoGen (Sinn, Germany). The gp130 monoclonal antibodies B-T2, B-P4 and B-P8 (Diaclone, Besançon, France) were generated as described elsewhere (Wijdenes et al., 1995). The monoclonal GFP antibody was obtained from Rockland (USA), the polyclonal pTyr-STAT3 antibody from New England Biolabs (Frankfurt, Germany) and the polyclonal STAT3 antibody from Santa Cruz (USA). Secondary antibodies were purchased from Dako (Hamburg, Germany). COS-7 simian monkey kidney cells (kindly provided by I. M. Kerr, Cancer Research UK, London, UK) and Hek293T cells (obtained from DSMZ, Braunschweig, Germany) were cultured in DMEM supplemented with 10% FCS, 100 mg/l streptomycin and 60 mg/l penicillin. Cells were grown at 37°C in a water-saturated atmosphere in 5% CO_2. High 5 (H5) cells (Invitrogen, USA) were cultured at 27°C. COS-7 cells were transfected using the DEAE-dextran method. Hek293T cells were transfected using FuGene (Roche Applied Science, Penzberg, Germany) according to the manufacturer's recommendations.

Cloning of expression vectors

The expression vectors pSVLgp130-CFP, pSVLgp130/id-CFP and pSVLgp130/id-YFP were cloned as described elsewhere (Giese et al., 2003). The construct pSBCLIFR/id-CFP is based on the earlier described expression vector pSBCLIFR (Timmermann et al., 2000) and encodes a cytoplasmically truncated LIFR protein in which Leu882 of the LIFR is followed by a Ser-Arg linker and Val2 of CFP. In the BiFC construct pSVLgp130/id-YC173, containing only the C-terminal half of YFP (amino acids 173-238), Asp173 of YFP immediately follows Pro668 of gp130. The BiFC constructs pSVLgp130/id-YN173 and pSBCLIFR/id-CN173 are derived from pSVLgp130/id-YFP and pSBCLIFR/id-CFP. pSVLgp130/id-YN173 and pSBCLIFR/id-CN173 contain the cDNA of N-terminal fragments (amino acids 2-172) of YFP (YN173) and CFP (CN173). The BiFC fragments of CFP and YFP were selected according to Hu and Kerppola (Hu and Kerppola, 2003). YFP-IL-6 was cloned by inserting the cDNA encoding YFP (Invitrogen, USA) between the signal sequence for secretion of the protein and the sequence encoding mature human IL-6 (Fig. 1A). All constructs were verified by DNA sequencing.

Purification and expression of YFP-IL-6 in insect cells

High 5 (H5) insect cells were cultured in Sf-900II medium (Gibco, USA) containing 2 μg/ml blasticidine. To stably transfect cells with the vector encoding YFP-IL-6, the Cellfectin method (Invitrogen, USA) was used. 72 hours after seeding of the transfected cells, supernatants were harvested and cleaned by centrifugation and sterile filtration. YFP-IL-6 was purified by affinity chromatography using immobilized sIL-6Rα. The eluate was dialyzed overnight against PBS (0.2 M NaCl, 2.5 mM KCl, 8 mM Na_2HPO_4, 1.5 mM KH_2PO_4). Purity and concentration of YFP-IL-6 in the eluted fractions was assessed by SDS-PAGE, western blotting, ELISA (Helle et al., 1991) and fluorescence spectroscopy.

SDS-PAGE and western blotting

Electrophoretically separated proteins were transferred to polyvinylidene difluoride membranes (PALL, Dreieich, Germany) by a semi-dry blotting procedure. The membrane was blocked with 10% bovine serum albumin, subsequently incubated with the antibodies as indicated in the figures and processed for chemiluminescence detection as described in the enhanced chemiluminescence manual (Amersham Biosciences, UK).

Immunofluorescence

Immunofluorescence staining of transfected COS-7 cells was carried out after formaldehyde fixation. The cells were blocked with PBS^{2+} (PBS with 1 mM $MgCl_2$ and 0.1 mM $CaCl_2$) containing 1% BSA for 30 minutes and then incubated with PBS^{2+} containing 0.1% BSA and the primary antibody (10 μg/ml) for 60 minutes. After washing twice with PBS^{2+} containing 0.1% BSA, the cells were incubated with a R-phycoerythrin-coupled secondary antibody at a 1:100 dilution in PBS^{2+} containing 0.1% BSA for 1 hour. After further washing with PBS^{2+} containing 0.1% BSA and afterwards with water, the slides were mounted with 10% (w/v) Mowiol (Calbiochem, USA), 25% (w/v) glycerin, 25% (v/v) water, 45% (v/v) 0.1 M Tris-HCl, pH 8.5.

Fixation of cells for FRET and BiFC detection

24 hours after transfection, cells were seeded on 18 mm glass coverslips and 48 hours after transfection cells were then fixed using 3% formaldehyde in PBS^{2+} (1 mM $MgCl_2$, 0.1 mM $CaCl_2$ in PBS) for 20 minutes. After fixation, cells were washed twice with PBS^{2+}, incubated for 5 minutes with PBS^{2+} containing 50 mM NH_4Cl, washed with PBS^{2+} and finally with water. The slides were mounted with Mowiol as described above. To support BiFC complementation, 30 hours after transfection the incubation temperature of Hek293T cells was decreased from 37°C to 30°C. After 18 hours of incubation at 30°C, the cells were fixed.

Confocal microscopy and live cell imaging

Confocal imaging was carried out on a Zeiss LSM 510 confocal microscope equipped with an argon-ion laser and a helium-neon laser (Zeiss, Jena, Germany). CFP and YFP signals were detected as described previously (Giese et al., 2003). Phycoerythrin (PE) fluorescence was detected using the 543 nm emission line of the helium-neon laser. A 543 nm dichroic mirror and a 560-640 nm bandpass filter completed the PE-beampath. For images of cells coexpressing CFP and YFP or CFP and PE the multi-track function of the LSM 510 was used. The images represent ~1-μm-thick confocal slices of whole cells. If not otherwise noted, cells were examined with a 63× 1.2 NA Zeiss water immersion objective.

Live cell imaging was carried out with COS-7 cells transiently transfected using the DEAE-dextran method. Transfected cells were grown on 18 mm glass coverslips. 48 hours after transfection the coverslips were placed in a home-built perfusion chamber and flushed with DMEM supplemented with 10% FCS, 100 mg/l streptomycin, and 60 mg/l penicillin. To maintain 37°C during all image acquisition the perfusion chamber and the objective were attached to a thermostat.

FRET detection

For FRET detection between CFP and YFP, a variant of the beampath for CFP detection was used with a 458/514 nm main dichroic mirror, a 515 nm dichroic mirror and a 530-600 nm bandpass filter to detect YFP fluorescence on a second photodetector in parallel to the CFP signal (bandpass 470-490 nm). The pinhole adjustment resulted in a 1.5 μm confocal slice. The image resolution was 256×256 pixels and 12-bit with a zoom factor of 2.6. After five prebleach scans of a region of interest (ROI 1) at the plasma membrane of the selected fixed cell, YFP in ROI 1 was bleached using the 514 nm argon laser line with 40% of 25 mW maximum laser power (100% transmission) for 100 iterations. Directly after bleaching of YFP the fluorescence was sampled in five postbleach scans. An additional ROI on the plasma membrane (ROI 2) was monitored in parallel to ROI 1 but was not bleached in order to detect fluorescence fluctuations independent of bleaching. A third ROI (ROI 3) was placed outside the cell to measure background fluorescence. The settings for prebleach and recovery image scans were 40% of 25 mW and 5% transmission for the 458 nm argon laser line. All images were acquired under the same settings for gain, resolution and optical components. Average fluorescence intensities within ROIs were exported into Microsoft Excel (Microsoft, USA). In each time series, the intensities in ROI 1 and ROI 2 were background corrected using the fluorescence intensities of ROI 3. The FRET energy transfer efficiency (E_f) was calculated as described (Karpova et al., 2003). For qualitative FRET imaging, before and after bleaching of YFP the whole cell was scanned using separate beampaths for CFP and YFP detection and the multitrack function of the LSM 510 as described under confocal microscopy.

BiFC detection

For measurement of YFP fluorescence after complementation of gp130/id-YC173 and gp130/id-YN173 the YFP beampath was used as described under confocal microscopy. According to Hu and Kerppola (Hu and Kerppola, 2003) complementation of the C-terminal YFP fragment YC173 with the N-terminal CFP fragment CN173 generates a fluorophore with an excitation maximum at 466 nm and an emission maximum at 497 nm. Therefore, fluorescence resulting from complementation of gp130/id-YC173 and LIFR/id-CN173 was detected using the 458 nm line of the argon laser in combination with a 458 nm main dichroic mirror and a 475 nm longpass filter. The spectra of the dyes were recorded with the Meta-detector (Zeiss, Jena, Germany) of the confocal microscope.

Images for quantitative BIFC analysis were collected using a 20× 0.75 NA Zeiss objective. The pinhole diameter resulted in 2 μm confocal slices. The images have a resolution of 512×512 pixels and a 12-bit intensity scale. All images were acquired under the same settings.

BiFC was also analysed by FACS. After fluorescence complementation, cells were washed with PBS and resuspended in PBS containing 5% FCS and 15 mM sodium azide on ice. FACS analysis was performed with a Facscalibur (Becton-Dickinson) using the 488 nm laser for excitation and a 515-545 nm bandpass filter for detection.

Evaluation of quantitative BiFC data

Images for quantitative BiFC analysis were filtered twice using a 7×7 pixel lowpass filter matrix. After subtraction of background fluorescence of image areas that were not covered with cells, the pixel quantities of the different fluorescence intensities of resulting images were exported into Microsoft Excel. The number of pixels representing BiFC fluorescence intensities was then related to the

amount of all pixels with fluorescence intensities produced by BiFC or autofluorescence of cells.

For all quantitative FRET and BiFC analyses, significance was calculated using one-way ANOVA including a Tamhane post-hoc test. Values of $P<0.05$ were considered significant.

Results

Binding of YFP-IL-6 to deletion mutants of gp130-CFP

If gp130 existed as a monomer in the plasma membrane, one binding epitope (D1 or the CBM) should be sufficient to recruit IL-6/sIL-6Rα complexes efficiently. To test this hypothesis we cloned a yellow fluorescent IL-6 (YFP-IL-6, Fig. 1A), a cyan fluorescent, internalization-deficient (id) gp130 (gp130/id-CFP) and deletion mutants thereof (gp130/ΔD1id-CFP, gp130/ΔD2,3id-CFP) (Fig. 2A, lower schemes). The cytoplasmic parts of the gp130/id constructs are deleted after Pro668. Therefore, the constructs lack the dileucine internalization motif (Dittrich et al., 1996) resulting in enhanced surface expression. Stimulation of Ba/F3-gp130-IL-6Rα cells with approximately equimolar amounts of YFP-IL-6 or IL-6 and subsequent analysis of STAT3 tyrosine phosphorylation (Fig. 1B) and cell proliferation (data not shown) revealed that the fusion of YFP does not interfere with the biological activity of the cytokine. Binding of YFP-IL-6 to COS-7 cells transfected with gp130/id-CFP strictly depends on the presence of sIL-6Rα, as COS-7 cells lack endogenous IL-6Rα (Fig. 1C).

The integrity of the gp130 deletion constructs was verified by the use of monoclonal antibodies that had been previously mapped to individual gp130 domains (Wijdenes et al., 1995). Whereas gp130/id-CFP is recognized by all three antibodies, antibodies directed against D1 and the CBM of gp130 fail to detect the corresponding deletion constructs (Fig. 2A). Furthermore, the immunofluorescence reveals that deletion of individual domains does not interfere with gp130 surface expression. Upon overexpression of gp130/id-CFP and the deletion constructs in COS-7 cells only the wild-type extracellular region recruits YFP-IL-6/sIL-6Rα complexes to the plasma membrane (Fig. 2B). Both deletion constructs failed to efficiently bind the ligand (Fig. 2C,D). Recruitment of IL-6/sIL-6Rα-complexes to monomeric gp130 would require binding of either IL-6 site II to the CBM of gp130 or IL-6 site III to D1 of gp130 as a first binding event. Neither of the two gp130 epitopes on its own efficiently recruits IL-6/sIL-6Rα complexes to the plasma membrane. Thus, preformation of gp130 homodimers would strongly increase the sensitivity of gp130 towards IL-6.

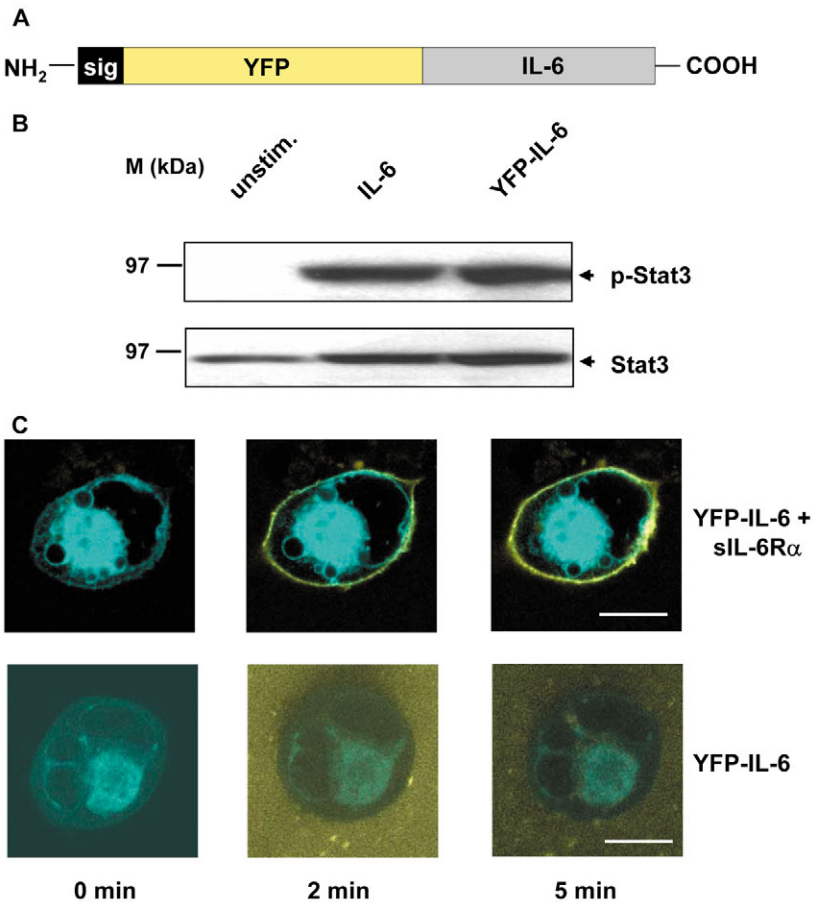

Fig. 1. Characterization of YFP-IL-6 and binding to gp130. (A) YFP-IL-6 consists of the signal sequence for secretion (black, 29 amino acids) followed by the YFP moiety (yellow, 238 amino acids) and mature human IL-6 (grey, 184 amino acids). (B) Ba/F3-gp130-IL-6Rα cells were left unstimulated or were stimulated for 15 minutes with 20 ng/ml IL-6 or 40 ng/ml purified YFP-IL-6. Phosphorylation of STAT3 was analysed by immunoblotting of cellular lysates using an antibody against tyrosine-phosphorylated STAT3. Equal loading was controlled using a STAT3 antibody. (C) COS-7 cells were transfected with an expression vector encoding gp130-CFP. 48 hours after transfection, confocal images from living cells incubated in a perfusion chamber at 37°C were taken using the YFP and CFP channels of the confocal microscope. Cells were stimulated with YFP-IL-6 (40 ng/ml) and sIL-6Rα (1 μg/ml) (upper row) or with YFP-IL-6 alone (lower row). Confocal images were taken at the time points indicated. Bar, 10 μm.

Detection of FRET at the plasma membrane by acceptor photobleaching

We adapted a previously published method (Karpova et al., 2003) to measure FRET between CFP and YFP by acceptor (YFP) photobleaching at the plasma membrane of single cells. Upon acceptor bleaching, the FRET donor (CFP) cannot transfer its energy to the acceptor any more and therefore its fluorescence increases. As a membrane-bound FRET positive control we fused a CFP-YFP in tandem to gp130 (gp130/id-C/YFP). This construct can be detected at the plasma membrane of transfected HEK293T cells in the YFP as well as in the CFP channel of the confocal microscope (Fig. 3A, left images). Selective bleaching of the YFP moiety with the 514 nm laser results in loss of YFP fluorescence and an increase in CFP fluorescence (Fig. 3A). The fluorescence intensities within the regions of interests (ROIs; e.g. white squares in Fig. 3A) of a series of images before and after bleaching are shown in the graph in Fig. 3B. The FRET

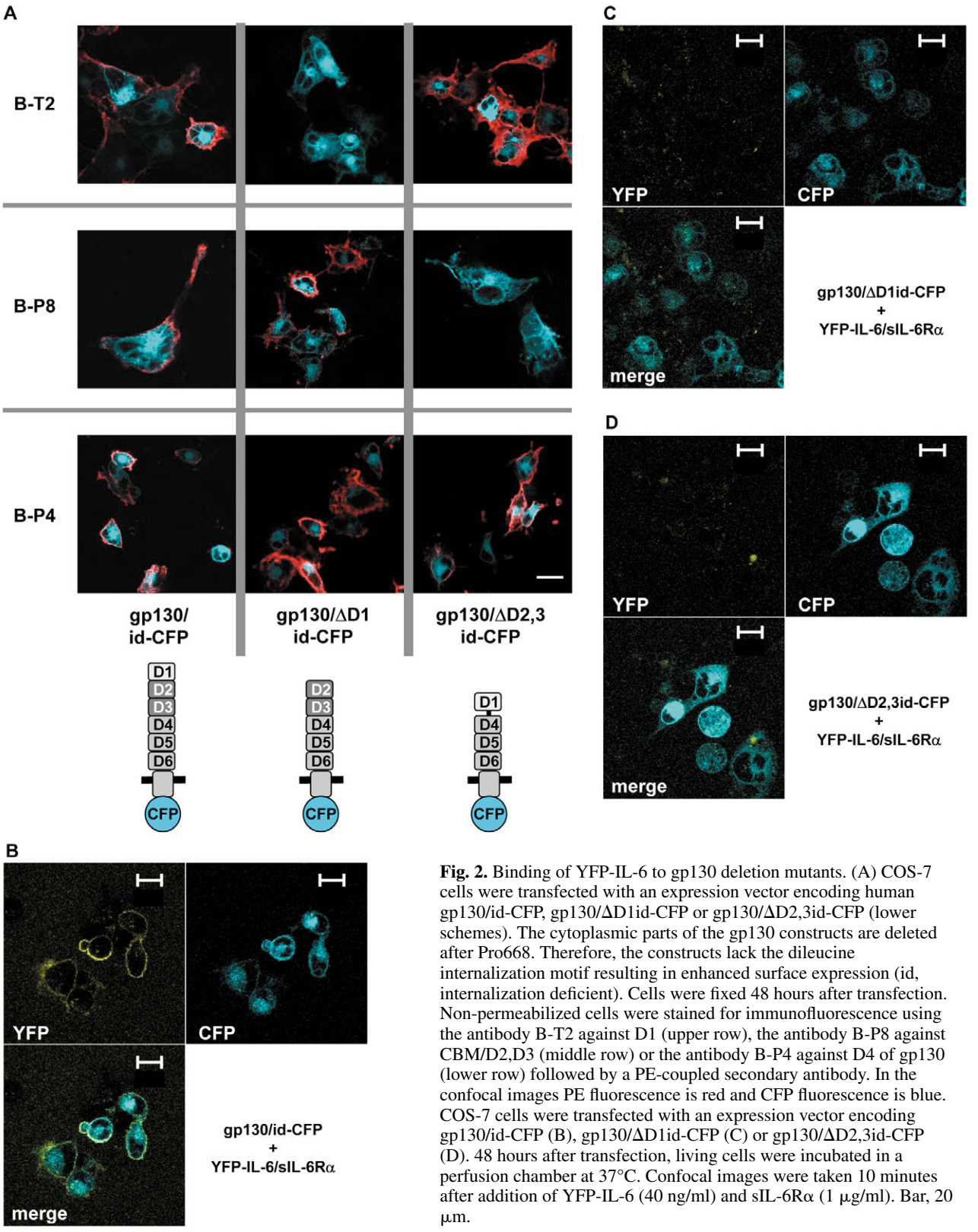

Fig. 2. Binding of YFP-IL-6 to gp130 deletion mutants. (A) COS-7 cells were transfected with an expression vector encoding human gp130/id-CFP, gp130/ΔD1id-CFP or gp130/ΔD2,3id-CFP (lower schemes). The cytoplasmic parts of the gp130 constructs are deleted after Pro668. Therefore, the constructs lack the dileucine internalization motif resulting in enhanced surface expression (id, internalization deficient). Cells were fixed 48 hours after transfection. Non-permeabilized cells were stained for immunofluorescence using the antibody B-T2 against D1 (upper row), the antibody B-P8 against CBM/D2,D3 (middle row) or the antibody B-P4 against D4 of gp130 (lower row) followed by a PE-coupled secondary antibody. In the confocal images PE fluorescence is red and CFP fluorescence is blue. COS-7 cells were transfected with an expression vector encoding gp130/id-CFP (B), gp130/ΔD1id-CFP (C) or gp130/ΔD2,3id-CFP (D). 48 hours after transfection, living cells were incubated in a perfusion chamber at 37°C. Confocal images were taken 10 minutes after addition of YFP-IL-6 (40 ng/ml) and sIL-6Rα (1 μg/ml). Bar, 20 μm.

efficiency can be calculated from the increase in CFP fluorescence after YFP bleaching (see Materials and Methods).

In a series of measurements, the FRET efficiencies of the FRET positive control (gp130/id-C/YFP) were compared with a FRET negative control (expression of gp130/id-CFP alone). A mean FRET efficiency of 29.8±3.6% was calculated for the gp130/id-C/YFP construct whereas the FRET negative control yielded values close to zero (Fig. 3C,D). The fluorescence

within the ROI before bleaching is a measure for the expression level of the fluorescent fusion proteins at the plasma membrane. The FRET efficiency of individual experiments is given as a function of the initial fluorescence (Fig. 3C). Notably, the FRET efficiency of gp130/id-C/YFP does not depend on the expression level.

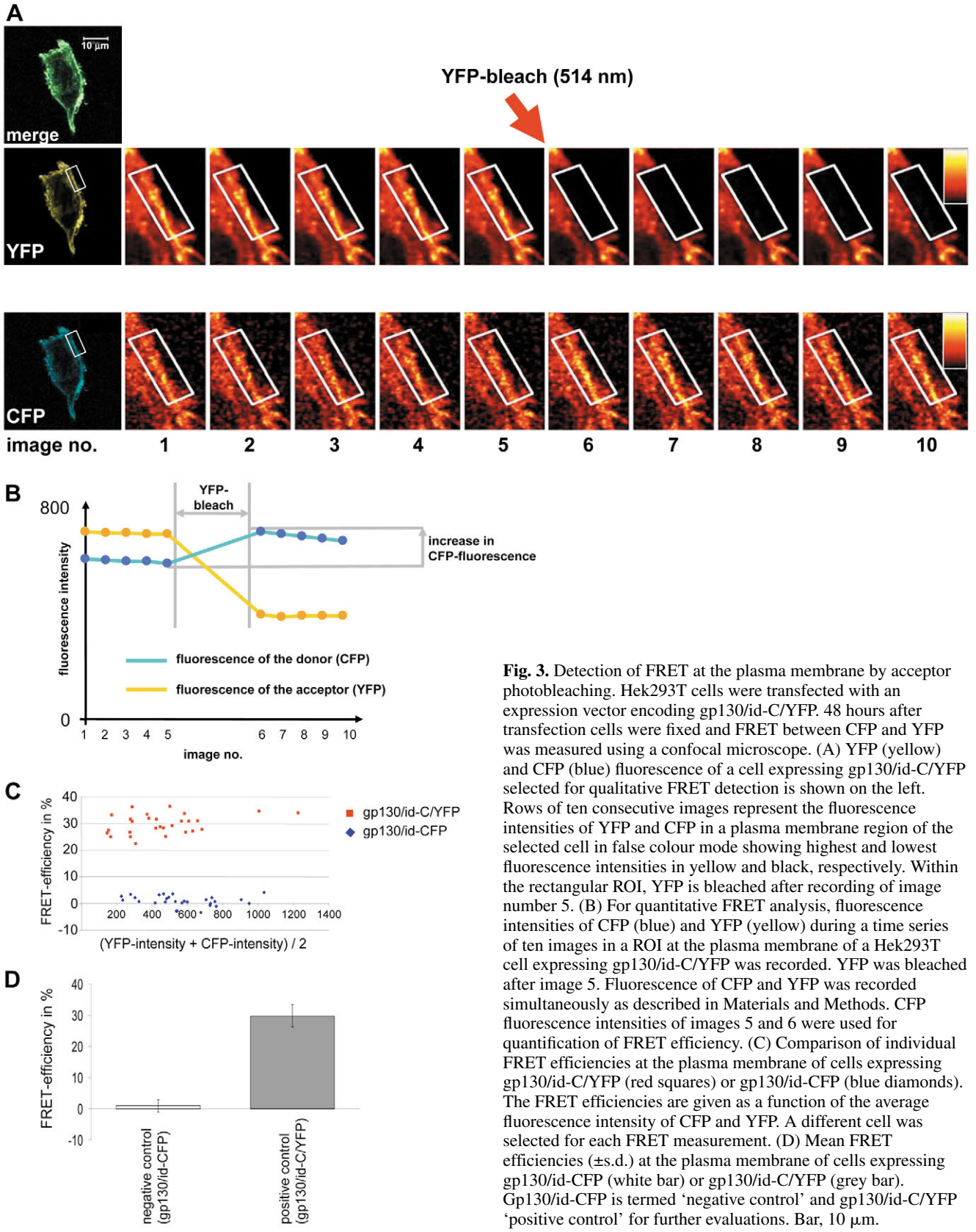

Fig. 3. Detection of FRET at the plasma membrane by acceptor photobleaching. Hek293T cells were transfected with an expression vector encoding gp130/id-C/YFP. 48 hours after transfection cells were fixed and FRET between CFP and YFP was measured using a confocal microscope. (A) YFP (yellow) and CFP (blue) fluorescence of a cell expressing gp130/id-C/YFP selected for qualitative FRET detection is shown on the left. Rows of ten consecutive images represent the fluorescence intensities of YFP and CFP in a plasma membrane region of the selected cell in false colour mode showing highest and lowest fluorescence intensities in yellow and black, respectively. Within the rectangular ROI, YFP is bleached after recording of image number 5. (B) For quantitative FRET analysis, fluorescence intensities of CFP (blue) and YFP (yellow) during a time series of ten images in a ROI at the plasma membrane of a Hek293T cell expressing gp130/id-C/YFP was recorded. YFP was bleached after image 5. Fluorescence of CFP and YFP was recorded simultaneously as described in Materials and Methods. CFP fluorescence intensities of images 5 and 6 were used for quantification of FRET efficiency. (C) Comparison of individual FRET efficiencies at the plasma membrane of cells expressing gp130/id-C/YFP (red squares) or gp130/id-CFP (blue diamonds). The FRET efficiencies are given as a function of the average fluorescence intensity of CFP and YFP. A different cell was selected for each FRET measurement. (D) Mean FRET efficiencies (±s.d.) at the plasma membrane of cells expressing gp130/id-CFP (white bar) or gp130/id-C/YFP (grey bar). Gp130/id-CFP is termed ‘negative control’ and gp130/id-C/YFP ‘positive control’ for further evaluations. Bar, 10 µm.

Analysis of gp130 homodimerization and gp130/LIFR heterodimerization by FRET

To detect gp130 homodimerization by FRET gp130/id-YFP and gp130/id-CFP expression vectors were cotransfected into HEK293T cells. For FRET analysis, only those cells where YFP expression equals or moderately exceeds CFP expression were considered (Fig. 4A, left diagram). The ratio of YFP intensity/CFP intensity of the gp130/id-C/YFP construct (not shown) providing equimolar YFP and CFP concentrations was used as a standard. A significant FRET signal could be detected which does not change upon stimulation with IL-6/sIL-6Rα complexes (Fig. 4A,B). The FRET signal slightly increases with elevated receptor expression (Fig. 4A, right diagram). The FRET approach is blind for gp130 homodimers with identical fluorophores and detects only dimers of gp130/id-YFP with gp130/id-CFP. Simple mendelian arithmetic revealed that this effect lowers the measured FRET values by 50%. This fact is considered in the bar chart (Fig. 4B) by depicting the hypothetical FRET values for exclusive YFP/CFP heterodimerization as dashed bars.

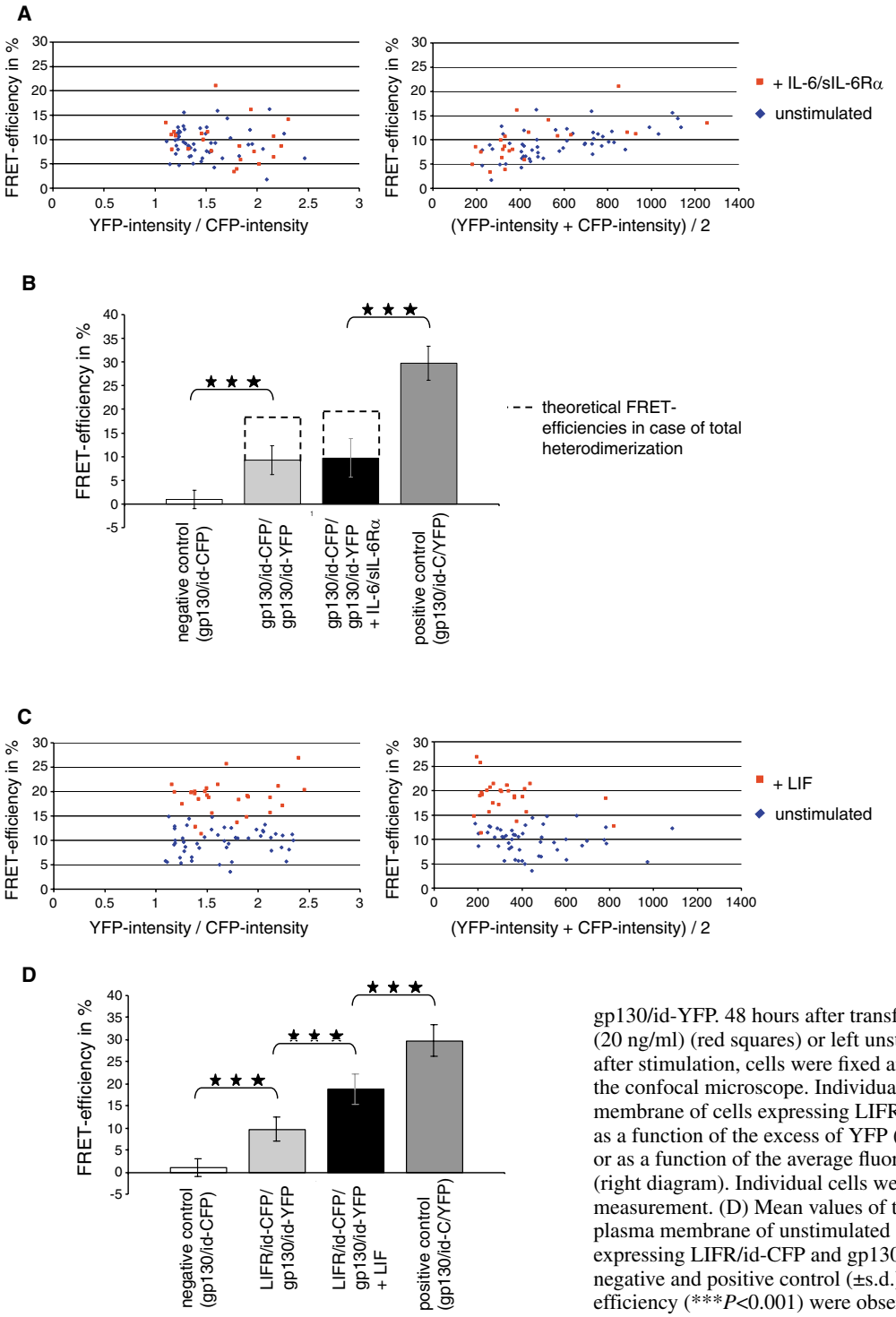

Fig. 4. Analysis of gp130 homodimerization and gp130/LIFR heterodimerization by FRET. (A) Hek293T cells were transfected with expression vectors encoding gp130/id-CFP and gp130/id-YFP. 48 hours after transfection, cells were stimulated with IL-6 (20 ng/ml) and sIL-6Rα (1 μg/ml) (red squares) or left unstimulated (blue diamonds). 15 minutes after stimulation, cells were fixed and analysed by quantitative FRET at the confocal microscope. Individual FRET efficiencies at the plasma membrane of cells expressing gp130/id-CFP and gp130/id-YFP are given as a function of the excess of YFP (acceptor) fluorescence (left) or as a function of the average fluorescence intensity of CFP and YFP (right). Individual cells were selected for each FRET measurement. (B) Mean values of the individual FRET efficiencies at the plasma membrane of unstimulated (light grey) or stimulated (black) cells expressing gp130/id-CFP and gp130/id-YFP in comparison to FRET negative and positive control (±s.d.). Significant differences (***P<0.001) in FRET efficiency were observed between experimental groups and the two control groups as indicated. Dashed bars represent the calculated FRET efficiencies for exclusive heterodimerization between CFP and YFP. (C) Hek293T cells were transfected with expression vectors encoding human LIFR/id-CFP and gp130/id-YFP. 48 hours after transfection, cells were stimulated with LIF (20 ng/ml) (red squares) or left unstimulated (blue diamonds). 15 minutes after stimulation, cells were fixed and analysed by quantitative FRET at the confocal microscope. Individual FRET efficiencies at the plasma membrane of cells expressing LIFR/id-CFP and gp130/id-YFP are given as a function of the excess of YFP (acceptor) fluorescence (left diagram) or as a function of the average fluorescence intensities of CFP and YFP (right diagram). Individual cells were selected for each FRET measurement. (D) Mean values of the individual FRET efficiencies at the plasma membrane of unstimulated (light grey) or stimulated (black) cells expressing LIFR/id-CFP and gp130/id-YFP in comparison to FRET negative and positive control (±s.d.). Significant differences in FRET efficiency (***P<0.001) were observed between groups as indicated.

In a similar approach, heterodimerization of gp130 with the LIFR was studied by coexpression of gp130/id-YFP with LIFR/id-CFP. The cytoplasmic part of the LIFR/id construct is truncated after Leu882 leading to deletion of the internalization motif (Thiel et al., 1999) and enhanced surface expression. Again, only those cells were considered where YFP expression equals or moderately exceeds CFP expression (Fig. 4C, left panel) As in the case of gp130 homodimerization, a FRET signal could be detected in unstimulated cells (Fig. 4C,D). As the two receptors are fused to different fluorophores, every gp130/LIFR heterodimer can be detected by the FRET approach. Most interestingly, the FRET signal strongly increases upon stimulation with LIF, indicating that the formation of gp130/LIFR heterodimers is induced by LIF (Fig. 4C,D). The FRET efficiency after LIF stimulation is in the same order of magnitude as the 'hypothetical' FRET efficiency of the gp130 homodimer (compare Fig. 4B, dashed bars and 4D). Taking this into account, in unstimulated cells gp130 preferentially forms gp130 homodimers. FRET efficiency of the gp130/LIFR heterodimer is independent of the expression levels (Fig. 4C, right panel).

Analysis of gp130 homodimerization and gp130/LIFR heterodimerization by BiFC

FRET does not discriminate between transient and stable interactions whereas the recently developed method of bimolecular fluorescence complementation (BiFC) detects predominantly stable protein-protein interactions (Hu et al., 2002). The BiFC method is based on the phenomenon that matching non-fluorescent 'halves' of fluorescent proteins can complement each other to form the intact fluorophore. For complementation to occur, an interaction of the halves is required that is in the range of several seconds (Hu et al., 2002). The affinity of the halves for each other is very low and therefore fluorescence complementation increases considerably by fusion partners that bring them into close proximity.

Gp130 was fused to the N-terminal half (gp130/id-YN173) or the C-terminal half of YFP (gp130/id-YC173). Cells were cotransfected with both constructs or with a single construct (gp130/id-YC173) as a negative control. As a first approach, we measured BiFC by FACS analysis. As reported previously (Kanno et al., 2004), the shifts of the cell populations are rather small owing to the low efficiency of fluorescence complementation. We detected a low BiFC fluorescence (Fig. 5A, dark grey) above background (light grey) in unstimulated cells that increased upon stimulation with IL-6/sIL-6Rα (black). In the same manner, heterodimerization of gp130 with the LIFR was analysed by cotransfection of gp130/id-YC173 and LIFR/id-CN173. Upon complementation, a YFP-CFP hybrid fluorophore is formed with specific spectral properties (Hu and Kerppola, 2003) which do not perfectly fit to the excitation/detection characteristics of a standard FACS device. Therefore, the shift of the population is even lower than in the case of gp130 BiFC. Nevertheless, a slight increase in fluorescence upon LIF stimulation is observed (Fig. 5D).

Next, we analysed BiFC triggered by gp130 homodimerization using the confocal microscope. Although the YFP fluorescence resulting from complementation is very weak, it could be clearly detected in the membranes of stimulated as well as unstimulated single cells (Fig. 5B, upper images). However, in the images taken at lower magnification it is visible that BiFC occurred more frequently in the stimulated cell population (Fig. 5B, lower images). We developed an algorithm (see Materials and Methods) to quantitatively evaluate BiFC from such microscopic images. We found a significant increase of BiFC fluorescence in cells transfected with the corresponding BiFC pair (gp130/id-YN173 and gp130/id-YC173) compared to cells expressing only a single half of YFP (gp130/id-YC173) (Fig. 5C). The fluorescence of the latter transfectants is due to autofluorescence of the cells. Upon stimulation with IL-6/sIL-6Rα the BiFC fluorescence significantly increased. Together with the FRET data, these findings suggest that IL-6/sIL-6Rα stimulation stabilizes a transient gp130 homodimer so that BiFC can occur. With the same approach, heterodimerization of gp130 with the LIFR was analysed by cotransfection of gp130/id-YC173 and LIFR/id-CN173. The beampath of the microscope was adjusted to the spectral properties of the hybrid fluorophore. As observed for the gp130 homodimer, BiFC is detectable in individual stimulated and unstimulated

Fig. 5. Analysis of gp130 homodimerization and gp130/LIFR heterodimerization by BiFC with confocal microscopy. (A) Hek293T cells were transfected with expression vectors encoding gp130/id-YC173 and gp130/id-YN173. Cells were incubated for 30 hours at 37°C, subsequently incubated for 18 hours at 30°C and afterwards analysed by FACS. 4 hours before temperature reduction, the cells were stimulated with IL-6 (20 ng/ml) and sIL-6Rα (1 μg/ml) or left unstimulated. Histograms represent unstimulated cells (dark grey), stimulated cells (black) or cells that expressed only gp130/id-YC173 (light grey). The scheme (right) depicts the complementation between the fragments of the fluorophores fused to gp130. (B) Hek293T cells were transfected and stimulated as described in A. Images of unstimulated (left) and stimulated cells (right) with high (upper row) and low magnification (lower row) were taken by using the YFP channel of the confocal microscope. (C) Proportion of the area of cells with BiFC fluorescence (A_{BiFC}) in the total cell covered area (A_{cells}) in low magnification images (n=30) of unstimulated cells (light grey), stimulated cells (dark grey) and cells that had expressed only gp130/id-YC173 (white) as a BiFC negative control (±s.d.). Significant differences in fluorescence ratio (***P<0.001) were observed between groups as indicated. (D) Hek293T cells were transfected with expression vectors encoding gp130/id-YC173 and LIFR/id-CN173. Cells were incubated for 30 hours at 37°C, subsequently incubated for 18 hours at 30°C and afterwards analysed by FACS. 4 hours before temperature reduction, the cells were stimulated with LIF (20 ng/ml) or left unstimulated. Histograms represent unstimulated cells (dark grey), stimulated cells (black) or cells that expressed only gp130/id-YC173 (light grey).The scheme (right) represents the complementation between the fragments of the fluorophores fused to LIFR and gp130. (E) Hek293T cells were transfected and stimulated as described in D. Images of unstimulated (left) and stimulated cells (right) under high (upper row) and low magnification (lower row) were taken using a channel of the confocal microscope adapted to the characteristics of the new fluorophore formed by YC173 and CN173 complementation. (F) Proportion of the cell area with BiFC fluorescence (A_{BiFC}) in the total cell covered area (A_{cells}) in low magnification images (n=30) of unstimulated cells (light grey), stimulated cells (dark grey) and cells that had expressed only gp130/id-YC173 (white) as a BiFC negative control (±s.d.). Significant differences in fluorescence ratio (*P<0.05 and ***P<0.001) were observed between groups as indicated. Bar, 10 μm (upper images in E,B); 100 μm (lower images in E,B).

cells (Fig. 5E, upper images). Upon LIF stimulation BiFC significantly increases (Fig. 5E, lower images and 5F).

Discussion

Activation of receptors by their ligands is the first step in cytokine signal transduction. Cytokine receptors belong to the family of receptors that span the membrane only once. For those types of receptors, ligand-induced receptor dimerization has been proposed to be the main mechanism for receptor activation. According to this model, formation of haematopoietic receptor complexes is based on two-dimensional Brownian diffusion-controlled collision of monomeric receptors (Wells and de Vos, 1996). Increasing evidence for preformed receptor dimers in the plasma membrane challenged this view. Preformed receptor oligomers have been described for several receptor systems such as EpoR (Livnah et al., 1999), IL-2R (Damjanovich et al., 1997) or TNFR (Chan et al., 2000). These observations suggest an alternative activation mechanism based on a switch of the conformation of a preformed receptor oligomer from an inactive to an active state triggered by the ligand.

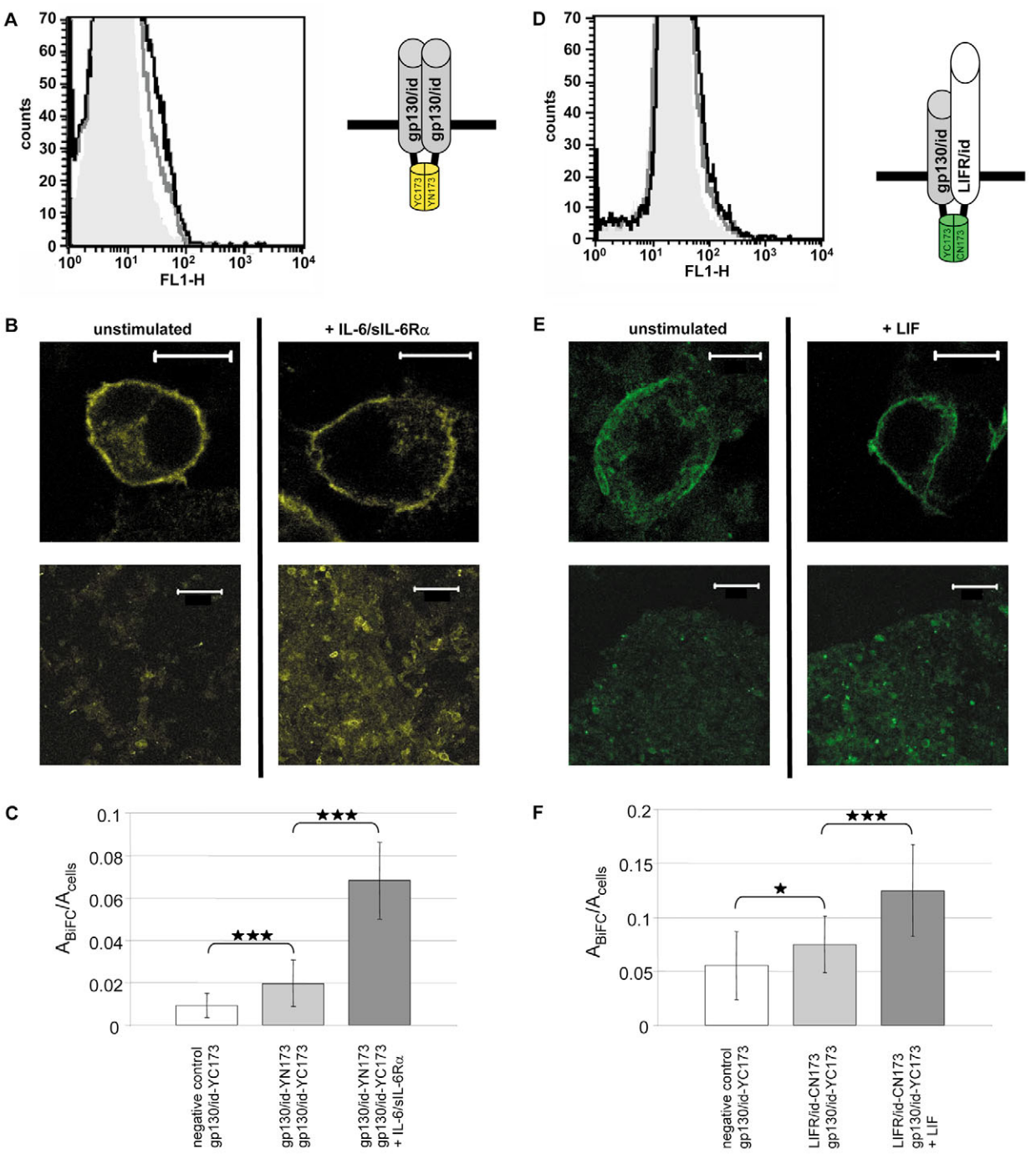

Fig. 5. See previous page for legend.

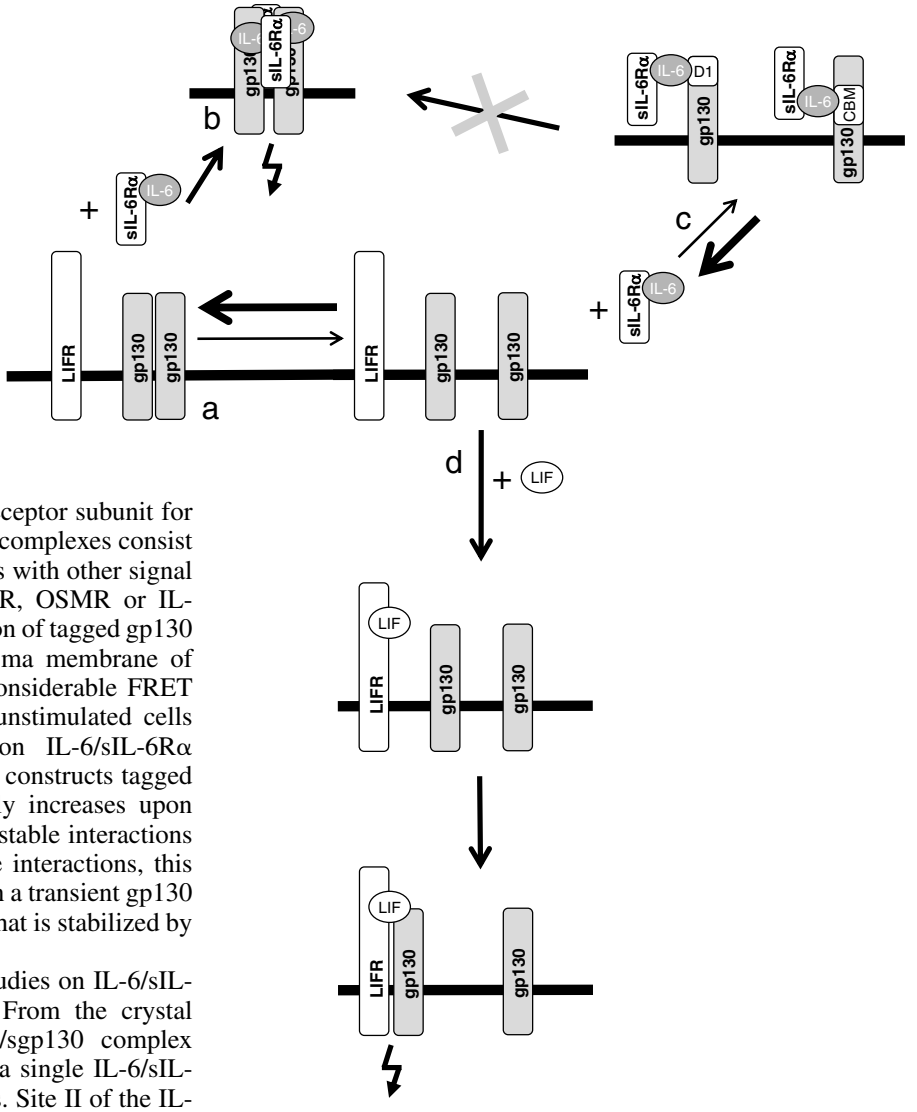

Fig. 6. Model for the dimerization of gp130 and LIFR. According to our data, a large portion of gp130 exists as a transient homodimer in the plasma membrane (a). This preformed homodimer is stabilized upon binding of IL-6/IL-6Rα complexes (b). Monomeric gp130 binds IL-6/IL-6Rα complexes less efficiently (c) and therefore only marginally contributes to IL-6-signalling. A gp130/LIFR heterodimer is formed mainly in response to LIF stimulation (d).

Gp130 is the shared signal transducing receptor subunit for the IL-6-type cytokines. Signalling receptor complexes consist of either gp130 homodimers or heterodimers with other signal transducing receptor subunits such as LIFR, OSMR or IL-27R/WSX-1. We investigated the dimerization of tagged gp130 and LIFR constructs by FRET at the plasma membrane of single cells and by BiFC. We detected a considerable FRET between CFP- and YFP-tagged gp130 in unstimulated cells that does not significantly increase upon IL-6/sIL-6Rα stimulation. However, BiFC between gp130 constructs tagged with corresponding halves of YFP strongly increases upon stimulation. As FRET detects transient and stable interactions whereas BiFC predominantly detects stable interactions, this finding can be explained by a model in which a transient gp130 homodimer is formed by weak interactions that is stabilized by binding of the ligand (Fig. 6b).

This interpretation is supported by our studies on IL-6/sIL-6Rα binding to gp130 deletion mutants. From the crystal structure of the hexameric IL-6/sIL-6Rα/sgp130 complex (Boulanger et al., 2003b) it is evident that a single IL-6/sIL-6Rα complex contacts two gp130 molecules. Site II of the IL-6/sIL-6Rα complex binds to the CBM (D2, D3) of one gp130 molecule, site III of the same IL-6/sIL-6Rα complex binds to D1 of the second gp130 molecule of the hexameric complex. As a consequence of gp130 monomers in the plasma membrane, in a first binding event IL-6/sIL-6Rα complexes would bind either to D1 or to the CBM of a single gp130 molecule. Our experiments with the respective deletion mutants show that neither of these binding epitopes alone efficiently recruits IL-6/sIL-6Rα-complexes to the plasma membrane (Fig. 6c). Thus, preformation of gp130 homodimers would greatly strengthen IL-6 sensing by the receptor by enabling IL-6/IL-6Rα complexes to bind to D1 and the CBM of two gp130 molecules simultaneously. This activation model requires that the preformed gp130 homodimers do not initiate signal transduction. Indeed, previous studies from our group have shown that dimerization of gp130 is not sufficient for signalling but that a defined conformation of the gp130 homodimer has to be adjusted by the ligand for signalling to occur (Greiser et al., 2002; Kurth et al., 2000; Müller-Newen et al., 2000).

Considering that in the case of ligand-independent pre-association there is no active involvement of the ligand in receptor dimerization, the ligand seems to be more important for complex stabilization and activation by a conformational change. If, as in the hexameric IL-6 receptor complex, several receptor chains constitute the complex, then pre-association represents a simplified method of complex formation. Complex preformation leads to greater ligand sensitivity because it prevents dissociation of the ligand from an intermediate low-affinity complex.

The tendency of LIFR to form heterodimers with gp130 in the absence of the ligand is rather low as FRET between CFP-tagged LIFR and YFP-tagged gp130 strongly increases upon LIF treatment. In line with this finding, BiFC between tagged LIFR and gp130 constructs increases significantly upon stimulation. Ligand-induced heterodimerization of LIFR and gp130 requires that LIFR or gp130 alone has a significant affinity to LIF. Binding of LIF to one receptor must have a sufficient half-life enabling this complex to encounter the second receptor by diffusion. In a recent study, it has been described that both gp130 and LIFR have measurable affinities to LIF (Boulanger et al., 2003a). As the affinity of LIF to the LIFR (K_d=1 nM) is higher than the affinity to the CBM of gp130 (K_d=80 nM), LIF binding to the LIFR might be the preferential first step in LIF signalling (Fig. 6, lower panel).

It is tempting to speculate how the other receptors involved in IL-6-type cytokine signalling fit into the scenario depicted in Fig. 6. It could be a general phenomenon that heterodimerization of gp130 with a second signal transducing receptor is triggered by the ligand. Thus, one would expect that heterodimerization of gp130 with the OSMR in response to OSM or of gp130 with the IL-27R/WSX-1 in response to IL-27 is ligand induced. At least for OSM it is known that it binds with sufficiently low affinity to gp130 alone (K_d=8 nM) (Gearing et al., 1992).

Signalling through gp130 homodimers requires binding of the cytokine to an α-receptor subunit that does not contribute to signalling. IL-6 binds to IL-6Rα and IL-11 binds to IL-11Rα. The membrane-bound α-receptors can be replaced by the corresponding soluble receptors. Therefore, pre-association of these receptors with gp130 is not a strict requirement for signalling. Nevertheless, one could imagine a pre-association of the membrane-bound α-receptor with gp130. So far, only preformed IL-6Rα homodimers have been described (Schuster et al., 2003).

Membrane-bound receptors are not the only preformed components of the Jak/STAT signalling pathway. It is well established that Janus kinases constitutively (Ihle, 1995) and stably (Giese et al., 2003) associate with cytokine receptors. In addition, proteins downstream of the receptors seem to exist in preformed complexes. Recent crystallographic evidence (Mao et al., 2005) supported the notion of STAT dimers formed prior to cytokine stimulation. Activation of STATs by tyrosine phosphorylation leads to rearrangement of the dimer and its stabilization. Thus, pre-association of signalling proteins seems to be a general mechanism to increase the sensitivity, specificity and speed of signalling pathways. The underlying protein-protein interactions are potential targets for the development of new drugs in order to treat diseases caused by dysregulated signal transduction pathways.

This work was supported by the Deutsche Forschungsgemeinschaft (Sonderforschungsbereich SFB 542 and Graduiertenkolleg Biointerface GRK 1035) and the Fonds der Chemischen Industrie (Frankfurt am Main). The authors thank John Wijdenes (Diaclone, Besançon, France) for the kind gift of the gp130 antibodies B-T2, B-P8 and B-P4, and Andrea Küster for excellent technical assistance.

References

Boulanger, M. J. and Garcia, K. C. (2004). Shared cytokine signaling receptors: structural insights from the gp130 system. *Adv. Protein Chem.* **68**, 107-146.

Boulanger, M. J., Bankovich, A. J., Kortemme, T., Baker, D. and Garcia, K. C. (2003a). Convergent mechanisms for recognition of divergent cytokines by the shared signaling receptor gp130. *Mol. Cell* **12**, 577-589.

Boulanger, M. J., Chow, D., Brevnova, E. E. and Garcia, K. C. (2003b). Hexameric structure and assembly of the interleukin-6/IL-6 α-receptor/gp130 complex. *Science* **300**, 2101-2104.

Boulay, J. L., O'Shea, J. J. and Paul, W. E. (2003). Molecular phylogeny within type I cytokines and their cognate receptors. *Immunity* **19**, 159-163.

Bravo, J. and Heath, J. K. (2000). Receptor recognition by gp130 cytokines. *EMBO J.* **19**, 2399-2411.

Chan, F. K., Chun, H. J., Zheng, L., Siegel, R. M., Bui, K. L. and Lenardo, M. J. (2000). A domain in TNF receptors that mediates ligand-independent receptor assembly and signaling. *Science* **288**, 2351-2354.

Damjanovich, S., Bene, L., Matko, J., Alileche, A., Goldman, C. K., Sharrow, S. and Waldmann, T. A. (1997). Preassembly of interleukin 2 (IL-2) receptor subunits on resting Kit 225 K6 T cells and their modulation by IL-2, IL-7, and IL-15: a fluorescence resonance energy transfer study. *Proc. Natl. Acad. Sci. USA* **94**, 13134-13139.

de Vos, A. M., Ultsch, M. and Kossiakoff, A. A. (1992). Human growth hormone and extracellular domain of its receptor: crystal structure of the complex. *Science* **255**, 306-312.

Dittrich, E, Haft, C. R., Muys, L., Heinrich, P. C. and Graeve, L. (1996). A di-leucine motif and an upstream serine in the interleukin-6 (IL-6) signal transducer gp130 mediate ligand-induced endocytosis and down-regulation of the IL-6 receptor. *J. Biol. Chem.* **271**, 5487-5494.

Gearing, D. P., Comeau, M. R., Friend, D. J., Gimpel, S. D., Thut, C. J., McGourty, J., Brasher, K. K., King, J. A., Gillis, S., Mosley, B. et al. (1992). The IL-6 signal transducer, gp130: an oncostatin M receptor and affinity converter for the LIF receptor. *Science* **255**, 1434-1437.

Giese, B., Au-Yeung, C.-K., Herrmann, A., Diefenbach, S., Haan, C., Küster, A., Wortmann, S. B., Roderburg, C., Heinrich, P. C., Behrmann, I. et al. (2003). Long-term association of the cytokine receptor gp130 and the Janus kinase Jak1 revealed by FRAP analysis. *J. Biol. Chem.* **278**, 39205-39213.

Greiser, J. S., Stross, C., Heinrich, P. C., Behrmann, I. and Hermanns, H. M. (2002). Orientational constraints of the gp130 intracellular juxtamembrane domain for signaling. *J. Biol. Chem.* **277**, 26959-26965.

Hammacher, A., Richardson, R. T., Layton, J. E., Smith, D. K., Angus, L. J. L., Hilton, D. J., Nicola, N. A., Wijdenes, J. and Simpson, R. J. (1998). The immunoglobulin-like module of gp130 is required for signaling by interleukin-6 but not by leukemia inhibitory factor. *J. Biol. Chem.* **273**, 22701-22707.

Heinrich, P. C., Behrmann, I., Haan, S., Hermanns, H. M., Müller-Newen, G. and Schaper, F. (2003). Principles of interleukin (IL)-6-type cytokine signalling and its regulation. *Biochem. J.* **374**, 1-20.

Helle, M., Boeije, L., de Groot, E., de Vos, A. and Aarden, L. (1991). Sensitive ELISA for interleukin-6. Detection of IL-6 in biological fluids: synovial fluids and sera. *J. Immunol. Meth.* **138**, 47-56.

Hibi, M., Murakami, M., Saito, M., Hirano, T., Taga, T. and Kishimoto, T. (1990). Molecular cloning and expression of an IL-6 signal transducer, gp130. *Cell* **63**, 1149-1157.

Hu, C. D. and Kerppola, T. K. (2003). Simultaneous visualization of multiple protein interactions in living cells using multicolor fluorescence complementation analysis. *Nat. Biotechnol.* **21**, 539-545.

Hu, C. D., Chinenov, Y. and Kerppola, T. K. (2002). Visualization of interactions among bZIP and Rel family proteins in living cells using bimolecular fluorescence complementation. *Mol. Cell* **9**, 789-798.

Ihle, J. N. (1995). Cytokine receptor signaling. *Nature* **377**, 591-594.

Jiang, G. and Hunter, T. (1999). Receptor signaling: when dimerization is not enough. *Curr. Biol.* **9**, R568-R571.

Kanno, T., Kanno, Y., Siegel, R. M., Jang, M. K., Lenardo, M. J. and Ozato, K. (2004). Selective recognition of acetylated histones by bromodomain proteins visualized in living cells. *Mol. Cell* **13**, 33-43.

Karpova, T. S., Baumann, C. T., He, L., Wu, X., Grammer, A., Lipsky, P., Hager, G. L. and McNally, J. G. (2003). Fluorescence resonance energy transfer from cyan to yellow fluorescent protein detected by acceptor photobleaching using confocal microscopy and a single laser. *J. Microsc.* **209**, 56-70.

Kurth, I., Horsten, U., Pflanz, S., Timmermann, A., Küster, A., Dahmen, H., Tacken, I., Heinrich, P. C. and Müller-Newen, G. (2000). Importance of the membrane-proximal extracellular domains for activation of the signal transducer glycoprotein 130. *J. Immunol.* **164**, 273-282.

Livnah, O., Johnson, D. L., Stura, E. A., Farrell, F. X., Barbone, F. P., You, Y., Liu, K. D., Goldsmith, M. A., He, W., Krause, C. D. et al. (1998). An antagonist peptide-EPO receptor complex suggests that receptor dimerization is not sufficient for activation. *Nat. Struct. Biol.* **5**, 993-1004.

Livnah, O., Stura, E. A., Middleton, S. A., Johnson, D. L., Jolliffe, L. K. and Wilson, I. A. (1999). Crystallographic evidence for preformed dimers of erythropoietin receptor before ligand activation. *Science* **283**, 987-990.

Mao, X., Ren, Z., Parker, G. N., Sondermann, H., Pastorello, M. A., Wang, W., McMurray, J. S., Demeler, B., Darnell, J. E., Jr and Chen, X. (2005). Structural bases of unphosphorylated STAT1 association and receptor binding. *Mol. Cell* **17**, 761-771.

Müller-Newen, G., Küster, A., Wijdenes, J., Schaper, F. and Heinrich, P. C. (2000). Studies on the IL-6-type cytokine signal transducer gp130 reveal a novel mechanism of receptor activation by monoclonal antibodies. *J. Biol. Chem.* **275**, 4579-4586.

Owczarek, C. M., Zhang, Y., Layton, M. J., Metcalf, D., Roberts, B. and Nicola, N. A. (1997). The unusual species cross-reactivity of the leukemia

inhibitory factor receptor alpha-chain is determined primarily by the immunoglobulin-like domain. *J. Biol. Chem.* **272**, 23976-23985.

Robb, L., Li, R., Hartley, L., Nandurkar, H. H., Koentgen, F. and Begley, C. G. (1998). Infertility in female mice lacking the receptor for interleukin 11 is due to a defective uterine response to implantation. *Nat. Med.* **4**, 303-308.

Schuster, B., Meinert, W., Rose-John, S. and Kallen, K. J. (2003). The human interleukin-6 (IL-6) receptor exists as a preformed dimer in the plasma membrane. *FEBS Lett.* **538**, 113-116.

Stewart, C. L., Kaspar, P., Brunet, L. J., Bhatt, H., Gadi, I., Kontgen, F. and Abbondanzo, S. J. (1992). Blastocyst implantation depends on maternal expression of leukaemia inhibitory factor. *Nature* **359**, 76-79.

Taga, T., Hibi, M., Hirata, Y., Yamasaki, K., Yasukawa, K., Matsuda, T., Hirano, T. and Kishimoto, T. (1989). Interleukin-6 triggers the association of its receptor with a possible signal transducer, gp130. *Cell* **58**, 573-581.

Thiel, S., Behrmann, I., Timmermann, A., Dahmen, H., Müller-Newen, G., Schaper, F., Tavernier, J., Pitard, V., Heinrich, P. C. and Graeve, L. (1999). Identification of a Leu-Ile interalization motif within the cytoplasmic domain of the leukaemia inhibitory factor receptor. *Biochem. J.* **339**, 15-19.

Timmermann, A., Pflanz, S., Grötzinger, J., Küster, A., Kurth, I., Pitard, V., Heinrich, P. C. and Müller-Newen, G. (2000). Different epitopes are required for gp130 activation by interleukin-6, oncostatin M and leukemia inhibitory factor. *FEBS Lett.* **468**, 120-124.

Wells, J. A. and de Vos, A. M. (1996). Hematopoietic receptor complexes. *Annu. Rev. Biochem.* **65**, 609-634.

Wijdenes, J., Heinrich, P. C., Müller-Newen, G., Roche, C., Zong-Jiang, G., Clement, C. and Klein, B. (1995). Interleukin-6 signal transducer gp130 has specific binding sites for different cytokines as determined by antagonistic and agonistic anti-gp130 monoclonal antibodies. *Eur. J. Immunol.* **25**, 3474-3481.

Yoshida, K., Taga, T., Saito, M., Suematsu, S., Kumanogoh, A., Tanaka, T., Fujiwara, H., Hirata, M., Yamagami, T., Nakahata, T. et al. (1996). Targeted disruption of gp130, the common signal transducer for the interleukin 6 family of cytokines, leads to myocardial and hematological disorders. *Proc. Natl. Acad. Sci. USA.* **93**, 407-411.